


Diversity in the organization of elastin bundles and intramembranous muscles in bat wings

Jorn A. Cheney,^{1,*} Justine J. Allen^{1,*}  and Sharon M. Swartz^{1,2} 

¹Department of Ecology and Evolutionary Biology, Brown University, Providence, RI, USA

²School of Engineering, Brown University, Providence, RI, USA

Abstract

Unlike birds and insects, bats fly with wings composed of thin skin that envelops the bones of the forelimb and spans the area between the limbs, digits, and sometimes the tail. This skin is complex and unusual; it is thinner than typical mammalian skin and contains organized bundles of elastin and embedded skeletal muscles. These elements are likely responsible for controlling the shape of the wing during flight and contributing to the aerodynamic capabilities of bats. We examined the arrangement of two macroscopic architectural elements in bat wings, elastin bundles and wing membrane muscles, to assess the diversity in bat wing skin morphology. We characterized the plagiopatagium and dactylopatagium of 130 species from 17 families of bats using cross-polarized light imaging. This method revealed structures with distinctive relative birefringence, heterogeneity of birefringence, variation in size, and degree of branching. We used previously published anatomical studies and tissue histology to identify birefringent structures, and we analyzed their architecture across taxa. Elastin bundles, muscles, neurovasculature, and collagenous fibers are present in all species. Elastin bundles are oriented in a predominantly spanwise or proximodistal direction, and there are five characteristic muscle arrays that occur within the plagiopatagium, far more muscle than typically recognized. These results inform recent functional studies of wing membrane architecture, support the functional hypothesis that elastin bundles aid wing folding and unfolding, and further suggest that all bats may use these architectural elements for flight. All species also possess numerous muscles within the wing membrane, but the architecture of muscle arrays within the plagiopatagium varies among families. To facilitate present and future discussion of these muscle arrays, we refine wing membrane muscle nomenclature in a manner that reflects this morphological diversity. The architecture of the constituents of the skin of the wing likely plays a key role in shaping wings during flight.

Key words: Chiroptera; muscle anatomy; plagiopatagiales; skin; wing membranes.

Introduction

The ecology and life history of bats (Order: Chiroptera) diverged from that of all other extant mammals when their ancestors evolved flapping wings composed of thin, membranous skin. More than 50 million years ago, the limbs of ancestral bats were exapted for use as wings (Gunnell & Simmons 2005). This adaptation allowed them to invade the skies and eventually exploit ecological niches as the only flapping flyers among mammals. Following the formation

of wings and the evolution of powered flight, bats underwent an explosive diversification (Teeling et al. 2005; Shi & Rabosky, 2015). Bats are the second-most speciose mammalian order; species range in body mass over three orders of magnitude (2 g to more than 1 kg), and vary in diet, habitat, wing morphology, and kinematics (Fenton & Simmons, 2014). Variation in these traits may place substantially different aerodynamic demands on the wings and therefore wing skin (Norberg & Rayner, 1987; Hedenström & Johansen, 2015; Swartz & Konow, 2015). Here, we document diversity among taxa in the architecture of key structural components, elastin bundles and membrane muscles, within the skin of the plagiopatagium (armwing) and dactylopatagium (handwing).

The skin of most of the bat body (e.g. head, abdomen, dorsum of the trunk, and foot pads) is typical of mammals, but that of the wings is distinctive (Sokolov, 1982; Madej et al. 2013). Wing skin has unique tissue-level morphology and is approximately an order of magnitude thinner than

Correspondence

Jorn A. Cheney, Department of Ecology and Evolutionary Biology, Brown University, Providence, RI 02912, USA. E: jcheney@rvc.ac.uk
Present address: Structure and Motion Lab, Royal Veterinary College, Hatfield AL9 7TA, UK

*Authors contributed equally on this project.

Accepted for publication 17 November 2016
Article published online 10 January 2017

body skin (~ 10 μm in the wing vs. 75–190 μm in the trunk for a 6 g bat; Madej et al. 2013). Further, wing skin possesses large, organized elastin bundles (ranging from tens to hundreds of microns in diameter), and skeletal muscles interspersed between the ventral and dorsal layers of the epidermis (Fig. 1A,B; Morra, 1899; Madej et al. 2013).

Elastin is generally found in skin as unorganized fibrils or mats (Meyer et al. 1994). In contrast, in bat wings, elastin fibrils are organized into abundant parallel-running, macroscopic bundles (Holbrook & Odland, 1978). In some other instances outside of skin, such as the ligamentum nuchae of some artiodactyls, elastin is also organized into large bundles comprising numerous parallel-organized fibrils (Dimery et al. 1985). Within mammalian skin, however, the absolute size of elastin bundles in bats is only clearly eclipsed by bundles in the ventral groove blubber of rorqual whales (Holbrook & Odland, 1978; Shadwick et al. 2013). Elastin behaves like many rubbers: it is highly extensible and resilient, capable of more than doubling in length and returning 90% of the strain energy stored (reviewed in Gosline et al. 2002). In bat wings, elastin bundles likely function to increase skin extensibility and recoil. Tensile tests along vs. perpendicular to the long axes of the bundles show greater extensibility and expansion of the compliant toe region of the stress-strain curve (Cheney et al. 2015). Combined with the high resilience of elastin,

these traits likely maintain membrane tension throughout the wingbeat cycle.

The muscles of the wing membrane are also unusual. They insert into wing membrane skin, with little or no direct attachment to bone. Elements of one group of these muscles, the plagiopatagiales proprii, both originate and insert within the wing skin. The plagiopatagiales proprii do not cross skeletal joints and are thus unlikely to control bone movement. Instead, this muscle group is hypothesized to modulate the effective stiffness of the wing membrane and thereby indirectly control wing camber (Cheney et al. 2014). Little is known about the details of morphology or function of the other wing membrane muscles. Various muscles have been observed in multiple species, and are described in several classic anatomical studies of bats, albeit with inconsistent nomenclature (Humphry, 1869; Schöbl, 1871; Macalister, 1872; Maisonneuve, 1878; Morra, 1899; Schumacher, 1932; Vaughan, 1959; Mori, 1960).

Here, we aimed to gain insight into the functional roles of elastin bundles and muscles in the wing membrane by examining diversity in the morphology of these components of the wing membrane using cross-polarized light imaging. We examined traits related to mechanical function, such as presence/absence, orientation, number, and size of muscles and elastin bundles. We were particularly interested in (i) whether the wing membranes of all bat species possess

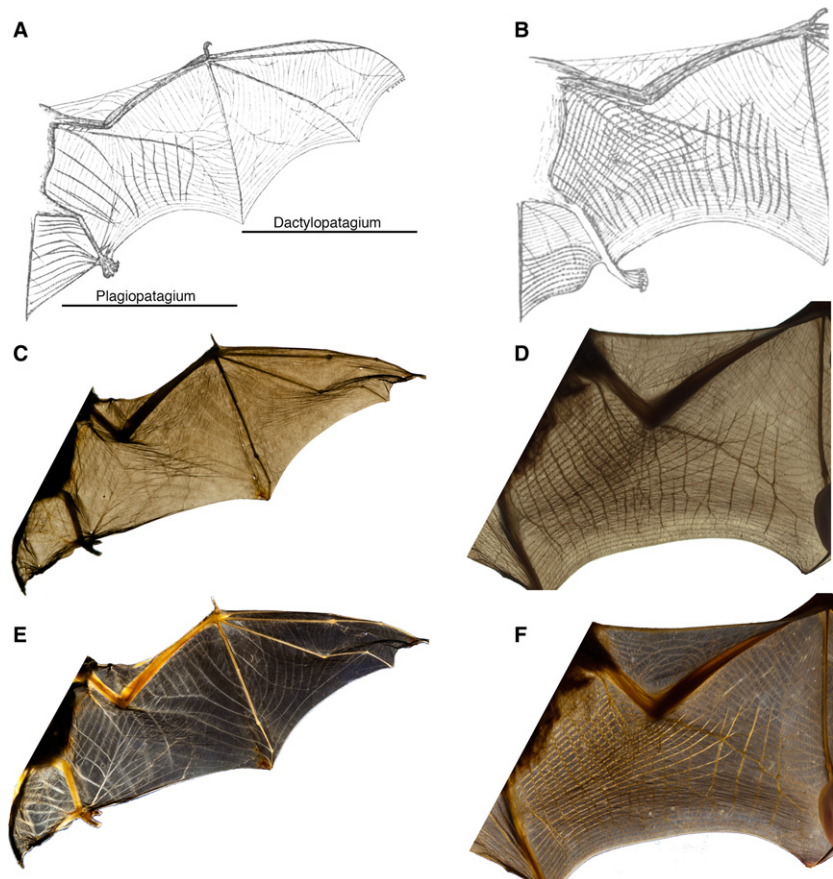


Fig. 1 Comparison of wing membrane structure differentiation using backlighting and cross-polarized light, referenced to previous anatomical study (Morra, 1899). Anatomical drawings of *Vespertilio murinus* (A; Vespertilionidae) and *Rhinolophus ferrumequinum* (B; Rhinolophidae) show elastin bundles as thin, gray lines and muscles as thick, striated lines. Backlighting the wing membrane (C,D) does not capture all of the described anatomical structures. Cross-polarized light (E,F) shows high contrast where elastin and muscle should occur, and the two tissues can be readily differentiated from one another. Species imaged are *Eptesicus fuscus* (C,E), and *Rhinolophus macrotus* (D,F).

elastin bundles and wing membrane muscles, and (ii) whether the architecture of elastin bundles across Chiroptera is consistent with the hypothesis that these bundles aid wing folding/unfolding, i.e. that the bundles run primarily along the wing's proximodistal or spanwise axis.

Materials and methods

Bats and tissue

Alcohol-preserved specimens of 130 species from 17 of the 18 families of bats were obtained from collections at the American Museum of Natural History, New York, the National Museum of Natural History, Washington, D.C., and the Field Museum, Chicago for imaging with cross-polarized light (Table 1).

Tissue used for histology was excised from one wing of one individual of each of the following species: *Artibeus lituratus* (Family: Phyllostomidae) and *Noctilio leporinus* (Noctilionidae), fixed in formalin and stored in 70% ethanol, and *Tadarida brasiliensis* (Molossidae), pinned taut and fixed in Hollande's fixative (Gray, 1954) for 200 h before being stored in 70% ethanol.

Cross-polarized light imaging

To investigate the arrangement of the elastin bundles and muscles within the bilayered skin of the wing, we employed cross-polarized light imaging. This technique takes advantage of the translucent and planar nature of the wing membrane. It is also beneficial because it is non-destructive, inexpensive, and relatively fast compared with histology or dissection. These characteristics allowed us

Table 1 Summary of species examined under cross-polarized light. We imaged 130 species from 17 families, distributed as indicated. Species and family designations are from Wilson & Reeder (2005), and phylogeny is from Teeling et al. (2005).

Family	Number of species imaged	
Pteropodidae	24	
Rhinolophidae	5	
Hipposideridae	4	
Megadermatidae	5	
Rhinopomatidae	2	
Emballonuridae	5	
Nycteridae	2	
Phyllostomidae	41	
Mormoopidae	4	
Noctilionidae	2	
Furipteridae	1	
Thyropteridae	1	
Mystacinidae	1	
Vespertilionidae	21	
Molossidae	8	
Natalidae	3	
Myzopodidae	1	

to sample many taxa, including those preserved as specimens in museum collections. Cross-polarized light imaging has not been used previously to study bat wing membrane morphology; previous studies relied upon standard backlighting for gross observation (Fig. 2; e.g. Gupta, 1967; Holbrook & Odland, 1978).

Cross-polarized light allows the differentiation of tissues based on birefringence that is the result of tissue composition and orientation relative to the polarization filters. In cross-polarized light imaging of thin biological structures such as skin, the tissue is back-illuminated using a light table covered with a polarization filter. The polarized light then passes through the tissue and the plane of polarization of light is rotated to varying degrees depending on the nature of the tissue. A second polarization filter placed above the tissue (i.e. between the tissue and the observer or imaging device), orthogonal to the first filter, allows only the rotated light to pass through the second filter. The amount of light that passes through the filters depends on the degree to which the light is orthogonal to the second filter. Image contrast depends on the relative birefringence of adjacent structures (e.g. Sankaran et al. 2002). Our system was composed of a light box (Porta-Trace 1012) covered with a linear polarizing film (TechSpec High Contrast linear polarizing film 250 × 250 mm; Edmund Optics Inc., Barrington, NJ, USA); images were captured with a DSLR camera (Nikon D300 or Olympus e-620) mounted with a macro lens and circular polarizing filter.

We stretched each wing over the light box for imaging. We captured images of the birefringent tissues at multiple orientations relative to the cross-polarization filters because the relative brightness of fibers depends on orientation. In addition, because museum specimens varied in preservation quality and wing extensibility, in some cases we imaged multiple individuals of a single species and/or compared closely related species.

Differentiating fiber populations

We anticipated that cross-polarized light imaging would accentuate highly ordered structures such as elastin bundles and muscles relative to the surrounding matrix. Both muscles and elastin bundles are sheathed in organized, birefringent collagen (Holbrook & Odland, 1978). Elastin is particularly birefringent when strained, as when the wing is unfolded, extended, and held flat in our imaging protocol (Cheney et al. 2015). In contrast, the tissue surrounding elastin bundles and muscles consists of thin dermis, composed, to a large extent, of randomly oriented collagen (Crowley & Hall, 1994), which produces little birefringence.

To determine whether this imaging method accurately differentiates elastin bundles, muscles, and the surrounding dermis, we compared images collected using cross-polarized light imaging with published anatomical descriptions and to histological sections of the wing membrane. Substantial, detailed, and relevant anatomical descriptions of the wing membrane exist only for *Rhinolophus ferrumequinum* and two species within Vespertilionidae (*Eptesicus serotinus* and *Vespertilio murinus*) (Schöbl, 1871; Morra, 1899). We also examined descriptions of a pteropodid (unspecified *Pteropus*; Schumacher, 1932), a molossid (*Eumops perotis*), and a phyllostomid (*Macrotus californicus*) (Vaughan, 1959). The species we imaged for comparison were those previously described or closely related species.

We excised samples for histology from species not previously described in detail to validate cross-polarized light imaging as a tissue differentiation technique. We selected sections (diagrammed in Fig. 3) of an unusual rostrocaudal or chordwise-oriented fiber within the dactylopatagium (Fig. 3, yellow); this fiber runs

Fig. 2 Cross-polarized light generally enhanced differentiation of wing membrane structures, but not for large bats. (A) Backlit plagiopatagium of *Glossophaga soricina* showed no presence of plagiopatagial muscle, but (B) cross-polarized light imaging differentiates chordwise structures consistent with plagiopatagial muscles (vertical bright fibers, yellow arrows). In large pteropodids only (C,D), cross-polarized light imaging reduced contrast of elastin bundles against skin. (C) Inset demonstrates the unusual crosshatched pattern of elastin bundles between digits V and IV seen in some pteropodids. Black bars: 5 cm.

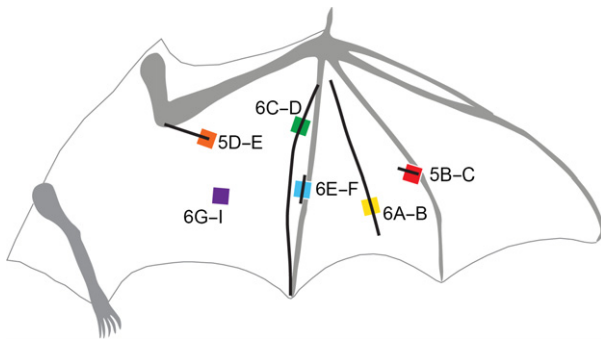
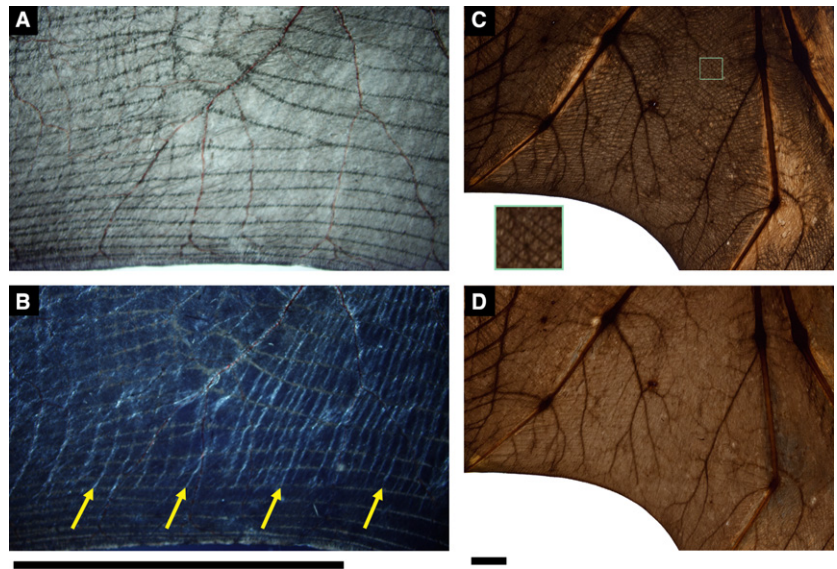


Fig. 3 Schematic showing the locations of samples excised for histological analysis: red, Fig. 5B–C; orange, Fig. 5D–E; yellow, Fig. 6A,B; green, Fig. 6C,D; light blue, Fig. 6E,F; purple, Fig. 6G,I.

orthogonal to the spanwise elastin network and appears distinctive in its birefringence: it is strongly birefringent when the spanwise fibers are weakly birefringent, and *vice versa*. However, when comparing maximum birefringence and other morphological traits, this fiber is similar to the spanwise bundles putatively composed of elastin. We also selected regions of the wing we expected to contain muscles and elastin bundles (Fig. 3, purple) or muscle and neurovasculature (Fig. 3, orange; putatively cubitopatagialis) for histological analysis. Additionally, we selected structures that appeared distinct from elastin, muscle, and neurovasculature in degree of birefringence, texture, and orientation, but which have not been described (Fig. 3, red, blue, and green). Two of these structures link elastin bundles to bone (Fig. 3, red and blue), and one is a highly birefringent chordwise fiber adjacent to digit V (Fig. 3, green). We see these structures in the wing membranes of species from many families. Further, because they appear distinct from elastin, muscle, and neurovasculature, we predicted that they are composed of organized collagen, similar to the structural composition of tendons or ligaments.

Histological samples were taken from *A. lituratus*, *T. brasiliensis*, and *N. leporinus*. For histological study, each tissue sample was dehydrated in an ethanol series and infiltrated with polyester wax (stock recipe: 90 g HallStar PEG 400 Distearate, MP: 36 °C combined

with 10 g 1-hexadecanol). Tissue was then oriented for sectioning and embedded in wax in BEEM® capsules. Serial sections (6 µm thick) were cut with a rotary microtome (Leica Biosystems or Spencer Lens Co.) and mounted on subbed glass slides (Weaver, 1955) with 2% paraformaldehyde. Sections were dewaxed and hydrated in an ethanol series and stained to differentiate elastin, collagen, and muscle using a modified Verhoeff's elastin stain and van Gieson's stain (Garvey et al. 1991) or Mallory's triple connective tissue stain (Humason, 1962) plus a differentiating step in a 0.5–1% acetic acid solution. Slides were dehydrated with two changes of 95% ethanol and one change of 100% ethanol, cleared with two changes of toluene, and coverslipped with mounting medium (Histomount; National Diagnostics). Sections were viewed with a microscope (Zeiss Axiovert or Nikon Eclipse E600) and imaged with a microscope-mounted digital camera (Canon EOS 5D mark II or Nikon DXM1200C). Tissues were identified by morphology and stain affinity.

Wing membrane architecture

We searched for elastin bundles, muscles, neurovascular bundles, and structures with distinct morphology observable under cross-polarized light. We assumed homology among muscles with similar anatomical attachments and orientation. Some structures had clear homologs across Chiroptera, but others did not. In particular, some of the muscle arrays of the wing membrane were more disparate than anticipated, hence we established definitions and consistent nomenclature for each muscle array. We provide descriptions of wing membrane architecture for Chiroptera as a whole for those features that are consistent in all or most families, and categorize other results by family, as appropriate.

Muscle nomenclature

Published anatomical studies have employed multiple, conflicting names for many wing membrane muscles. We synthesized the various names and followed an 'origin-insertion' convention; this convention has been used frequently for the wing membrane muscles (e.g. Humphry, 1869; Macalister, 1872) and preserves the names of

the most commonly discussed muscles. We found that, in general, details of muscle origins were often consistent at the level of families or groups of families, but, in some cases, varied within families or even genera. Our nomenclature reflects a general region of origin and not a highly specific attachment site.

Results

Polarized light validation

The birefringent fibers in the wing membrane varied in morphology, and the majority segregate into three populations according to differences in relative brightness, heterogeneity of brightness, variation in size, and degree of branching. Comparison of previously published anatomical drawings of the wing membrane with images acquired using cross-polarized light imaging supported our segregation of populations, and helped discern tissue types. The three predominant fiber populations were elastin bundles, muscles, and neurovascular bundles (Morra, 1899; Schöbl, 1871; Schumacher, 1932; Figs 1 and 4). We also observed birefringent fibers with properties not consistent with these three tissue types, which were not included in previously published anatomical drawings (most clearly highlighted in Figs 5A and 6C,E). These distinct fiber populations could be seen in many species, but they represent a small fraction of the total structures within the wing membrane (Fig. 4, dashed green lines).

Histology further validated the use of cross-polarized light as a technique for tissue differentiation. Our histological analysis confirmed the identity of putative elastin (Figs 5D and 6B,H,I), muscle (Figs 5D and 6H,I), neurovasculature (Fig. 5D), and unusual birefringent fibers distinct in composition (Figs 5B and 6D,F). From tissue specimens of an *A. lituratus*, we determined that the unusual chordwise-oriented structure observed between digits V and IV in the dactylopatagium of some species is a bundle of elastin (Fig. 3, yellow; Fig. 6A,B). In the same specimen, we found, as expected, muscle and elastin in a number of tissue samples, organized in a gridlike pattern (Fig. 6H,I). In *T. brasiliensis*, a tissue distal to the elbow was expected to contain muscle and neurovasculature only, based on cross-polarized light, but it was found additionally to contain elastin (Fig. 5D). In this case, the elastin bundle was not distinguished from the muscle or neurovascular bundle because it is immediately deep to highly birefringent muscle (cubitopatagialis).

The three samples with highly birefringent fibers of unknown composition (Fig. 3, red, blue, and green) each contained bundles of organized collagen (Figs 5B and 6F,D, respectively) and represent tissues that occur in several locations in the wing, at differing orientations. Two of these collagen bundles formed the distal insertion site for elastin bundles in *N. leporinus* and *A. lituratus* (Figs 5A and 6E). Similar bundles are visible between elastin bundles and bones in many other, especially larger-bodied, species. The

third sample was from a distinctive chordwise-running fiber proximal to digit V (Fig 3, green; Fig. 6C). Although we did not deliberately image wings for birefringent fibers consistent with collagen bundles, they were visible in at least one representative of every family except for Thyropteridae (Fig. 4, green lines).

When illuminated with cross-polarized light, elastin bundles appear weakly birefringent. This birefringence is relatively consistent among elastin bundles and along the length of individual bundles (Fig. 4). Elastin bundles are not tortuous, often branch, and maintain a consistent thickness along their length. Elastin bundles occur in the plagiopatagium and dactylopatagium in all species, and in the propatagium and uropatagium in at least some species, although those regions of the wing were not studied in detail here.

Muscles are generally larger and more birefringent than elastin bundles, and their birefringence is heterogeneous along the length of the muscle belly (Fig. 4). Muscles also possess tapering ends and branch infrequently. They occur only in the plagiopatagium, propatagium, and uropatagium (the latter two regions were not part of this study). There are no muscles in the dactylopatagium.

Neurovascular bundles are moderately birefringent, heterogeneous in birefringence, and follow a tortuous path (Fig. 4). They frequently occur adjacent to muscle bellies and branch frequently, decreasing in diameter with each branch. They occur in all parts of the wing membrane.

In bats larger than approximately 200 g (pteropodids only in this sample), cross-polarized light is less effective than non-polarized light (i.e. standard backlighting) in differentiating elastin bundles from surrounding tissue (Fig. 2). For species with smaller body sizes, typical of most chiropterans, cross-polarized light provides enhanced contrast, facilitates observation of known wing structures, and reveals the presence of additional structures otherwise not readily visible. For example, with standard backlighting and dissection, plagiopatagiales proprii were not observed in *Eptesicus fuscus* (Gupta, 1967), or *Glossophaga soricina*, but were easily identifiable in these species when back-illuminated with cross-polarized light (Fig. 2).

Wing membrane diversity: elastin

Elastin bundles run primarily in parallel and are oriented approximately proximodistally (spanwise) along the axis of folding and unfolding. We observed this pattern in all families we studied and found that it is typical of both the plagiopatagium and dactylopatagium. Although this general pattern is consistent, localized regions of the wing revealed variation in elastin bundle density, branching frequency, and bundle angle among species.

Most of the variation in elastin network architecture occurs in three anatomical locations: (i) immediately adjacent to the skeleton of the digits; (ii) approximately mid-way between metacarpals V and VI; and (iii) in the

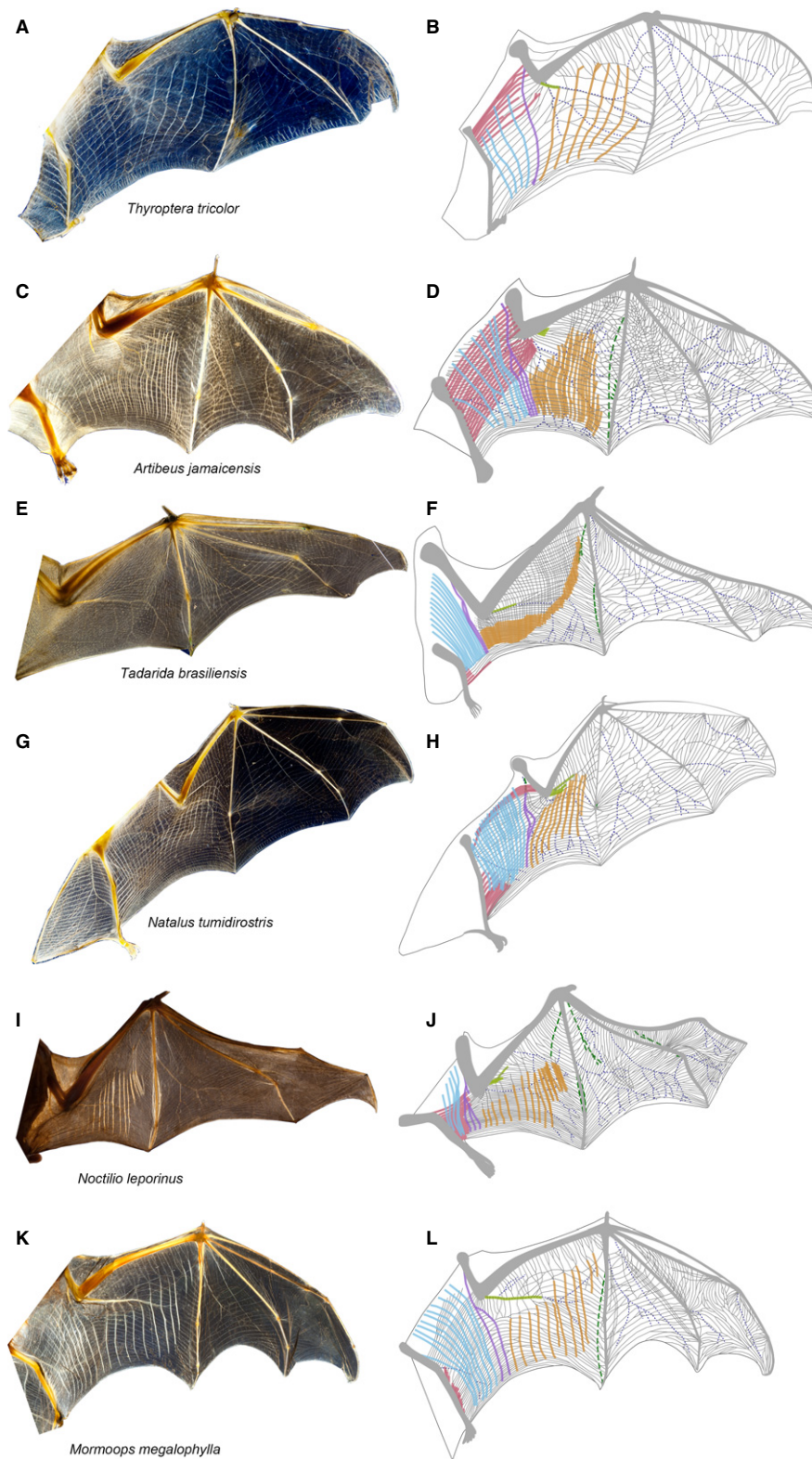


Fig. 4 Diversity in wing membrane architecture. Cross-polarized light images and schematics showing elastin bundles (gray lines), muscle arrays (solid colored lines), neurovasculature (dashed blue lines), and collagenous fiber bundles (dashed green lines). Schematics were developed using multiple cross-polarized light images. Muscle arrays are tibiopatagiales (red), dorsopatagiales (blue), coracopatagiales (purple), plagiopatagiales proprii (orange), cubitopatagiales (green). Families: (A,B) Thyropteridae; (C,D) Phyllostomidae; (E,F) Molossidae; (G,H) Natalidae; (I,J) Noctilionidae; (K,L) Mormoopidae.

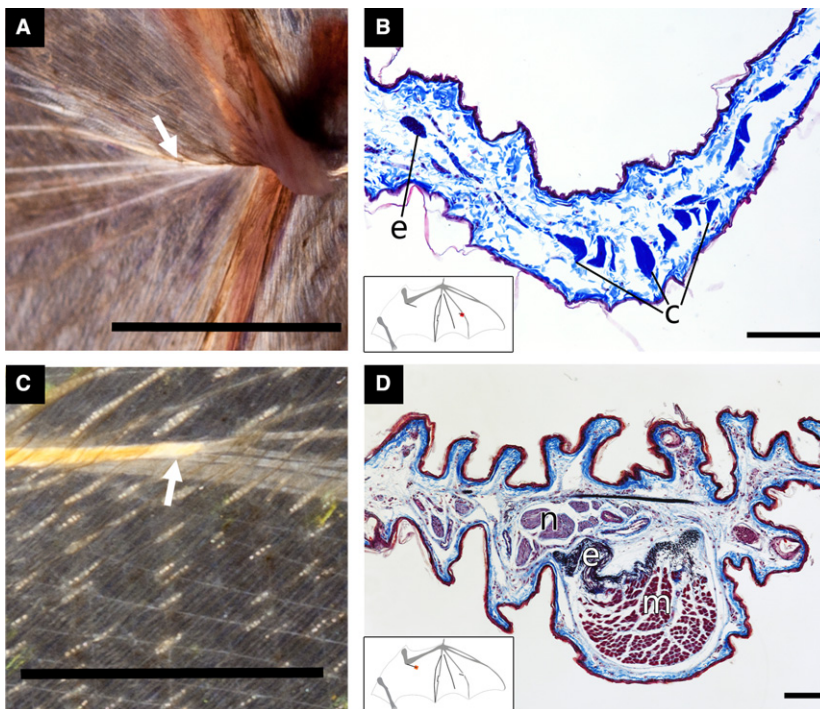


Fig. 5 Cross-polarized light images of distinct tissues identified with histology. (A,C) Images of the wing skin taken using cross-polarized light. (B,D) Light micrographs of tissue samples oriented dorsal side up and stained with modified Verhoeff's elastin stain and Mallory's triple connective tissue stain; collagen, blue; elastin, dark purple to navy; nerves, light purple. (A,B) Tissue sample from *Noctilio leporinus*; convergent elastin bundles immediately proximal to the metacarpophalangeal joint of digit IV appear to attach to the joint via a collagenous ligament. (C,D) Tissue sample from *Tadarida brasiliensis*; fibers proximal to the elbow are composed of muscle (cubitopatagialis) and elastin. Tissue types were identified by morphology and stain affinity: c, collagen; e, elastin; m, muscle; and n, nerve. Scale bars: (A) ~ 1 cm; (B,D) 100 μ m; (C) ~ 0.5 cm.

rostrorodistal plagiopatagium, between the forearm and metacarpal V and rostral to the plagiopatagiales proprii. Adjacent to the digits, elastin bundles frequently branch and fuse, except at skeletal joints, where elastin bundles often converge (Fig. 4). Between metacarpals V and IV in Myzopodidae and some Phyllostomidae, elastin bundles frequently intersect at angles, resulting in a reticulated or honeycomb-like pattern (Fig. 4D). In approximately the same region of the dactylopatagium in Pteropodidae, two populations of elastin bundles form a grid oriented at about $\pm 45^\circ$ to the spanwise axis (Fig. 2C, inset). Between the radius and metacarpal V, elastin bundles can cross in the distal plagiopatagium, rostral to the plagiopatagiales proprii. There, two populations of elastin bundles occur, one oriented spanwise and the other approximately rostrocaudal or chordwise. We observed this cross-hatched pattern of elastin bundles (Fig. 4D,F) in Emballonuridae, Pteropodidae, Rhinopomatidae, Mystacinidae, Molossidae, and some Hipposideridae and Phyllostomidae.

There is variation in elastin network architecture in additional small regions of the wing in some species. For example, in *Mormoops megalophylla*, but not in two other mormoopids in our sample (both from the genus *Pteronotus*), elastin bundles converge toward the wingtip (Fig. 4L). In *N. leporinus*, a similar radiating arrangement of elastin bundles occurs near the center of the dactylopatagium between digits V and IV (Fig. 4J). Finally, in several species, elastin bundle architecture deviates from the general spanwise network to form local arcades originating from a central point, particularly adjacent to the digits, as in the dactylopatagium of Mormoopidae (Fig. 4L).

Wing membrane diversity: muscle

We propose muscle nomenclature that employs an 'origin-insertion' convention to aid the identification and discussion of the muscles that attach within the plagiopatagium. The origins of muscle arrays in the plagiopatagium are often extensive, potentially including multiple structures, although the extent of attachment varies. Each individual muscle belly typically has a discrete and localized origin, but the array of multiple, distinct muscle bellies often originates from various locations along the bone(s). For this reason, we ascribe origin to an anatomical region and not a single localized site (Fig. 4). Muscles originate from the (i) dorsum of the trunk, (ii) axillary region, particularly the scapula, (iii) plagiopatagium, (iv) cubital region (elbow), and (v) tibia and adjacent structures, particularly the distal femur and proximal tarsus. We designate these muscle groups (i) mm. dorsopatagiales, (ii) mm. coracopatagiales, (iii) mm. plagiopatagiales proprii, (iv) mm. cubitopatagiales, and (v) mm. tibioapatagiales. This naming convention is close to that of Schumacher (1932) in the first three cases, although we have abbreviated the insertion from the specific 'plagiopatagium' to the more general 'patagium' for brevity.

Muscle architecture in the plagiopatagium exhibits many different patterns (Supporting Information Table S1). In particular, we observed variation in number, relative length and width, and orientation of muscle bellies (Fig. 4). We report observations of muscle presence; however, conclusive determination of muscle absence requires thorough histological examination. We describe each muscle group below.

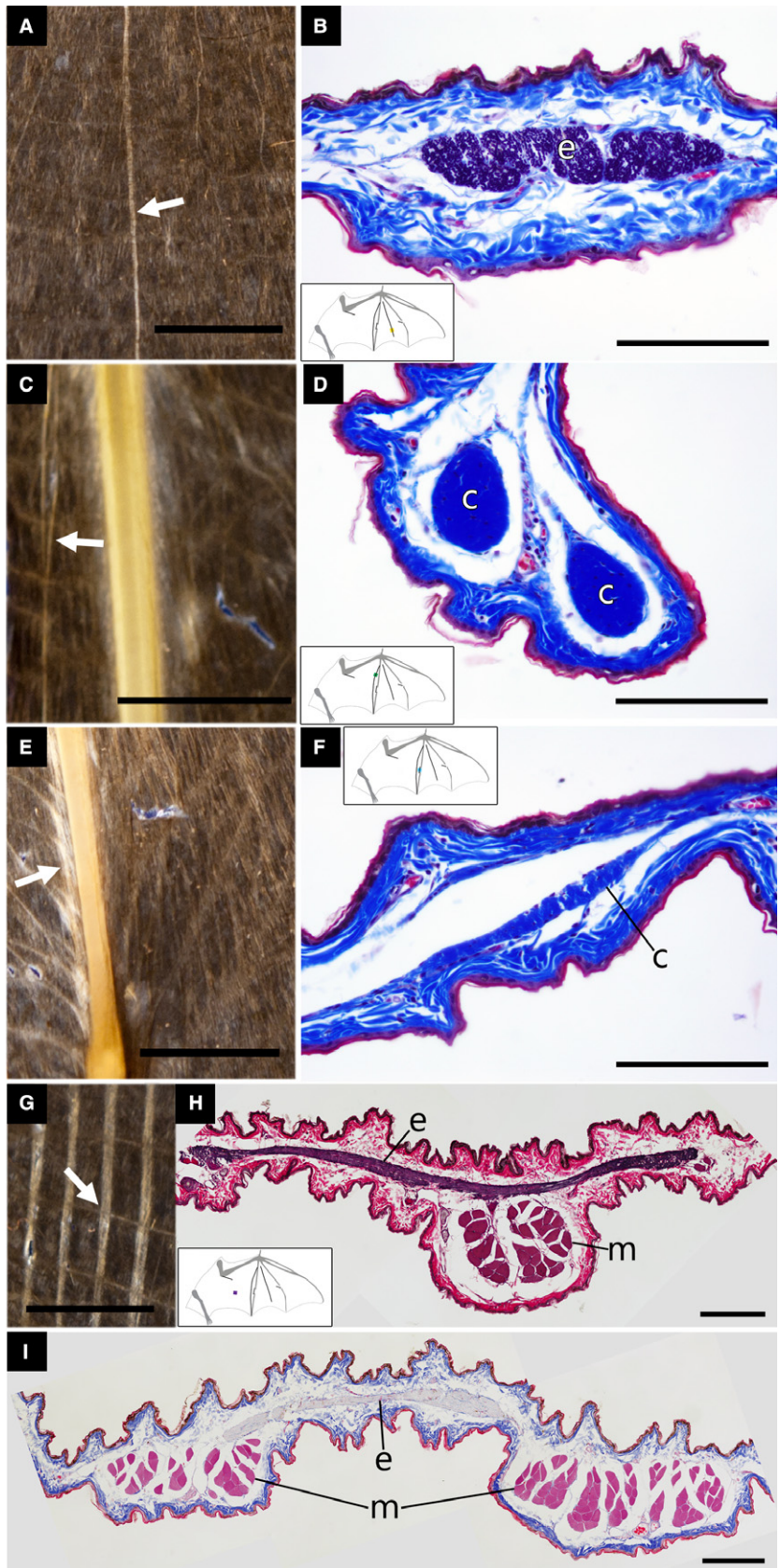


Fig. 6 Tissue samples taken from *Artibeus lituratus*. (A,C,E,G) Images taken using cross-polarized light showing the ventral surface of the wing skin. (B,D,F,H,I) Light micrographs of tissue samples oriented dorsal side up and stained with various histological stains: (B,D,F) modified Verhoeff's elastin stain and Mallory's triple connective tissue stain; blood cells, pink; collagen, blue; elastin, dark purple to navy (H) modified Verhoeff's elastin stain and Van Gieson's stain; collagen, pink; elastin, dark purple; muscle, red (I) Mallory's triple connective tissue stain; blood cells, bright pink; collagen, blue; elastin, unstained; muscle, pink. (A,B) The interdigital fiber between digits V and VI is composed of elastin. (C,D) The fiber just proximal to digit V is a collagenous ligament. (E,F) The highly birefringent fibers adjacent to digit V are collagenous and appear to connect spanwise elastin bundles to the digit. (G–I) The plagiopatagiales proprii muscles run rostrocaudally and approximately perpendicular to spanwise elastin bundles. Tissue types were identified by morphology and stain affinity: e, elastin; c, collagen; and m, muscle. Scale bars: (A,C,E,G) ~ 1 cm; (B,D,F,H,I) 100 μm.

Tibiopatagiales

The tibiopatagiales most commonly originate from the leg, but muscles in this group also originate from the distal femur or proximal portions of the tarsus. We did not observe tibiopatagiales in Pteropodidae, Emballonuridae, Nycteridae, Furipteridae or Myzopodidae. When present, they run laterally and, when of substantial length, rostrally. Muscle length relative to plagiopatagium length varies, and our observations of relative lengths showed a discontinuous distribution with three categories: (i) very short (< 10% of plagiopatagium length; e.g. Fig. 4H), (ii) moderately long, extending to the elbow, or (iii) long, extending across the span of the plagiopatagium. For all species within a given family, tibiopatagiales lengths fell into a single category except within Phyllostomidae, where some species have moderately long and others long muscles (Fig. 4D depicts muscles of moderate length). In species with observable tibiopatagiales, we observed between seven and 25 muscles.

Dorsopatagiales

The dorsopatagiales, observed in all families, enter the wing membrane from the thorax and abdomen and run latero-caudally. These muscles insert into the plagiopatagium just rostral to the trailing edge. The density of these muscles varies substantially and is typically similar to that of the plagiopatagiales proprii. *Mystacina tuberculata* and some of the Megadermatidae possess only a single dorsopatagialis.

Coracopatagiales

The coracopatagiales arise in the axillary region, but their precise attachment points could not be observed with certainty. These muscles typically traverse the axilla to the plagiopatagium as a single muscle bundle, but in some species, branch distally into multiple bellies (e.g. Fig. 4B vs. D). The muscles run approximately caudally and terminate near the trailing edge. They form a boundary between the proximal dorsopatagiales and the distal plagiopatagiales proprii. We observed these muscles in all families except Mystacinidae, a family in which skin in the axillary region is exceptionally thick and unusually wrinkled, which obscured imaging.

Plagiopatagiales proprii

The plagiopatagiales proprii originate and insert within the plagiopatagium, and run rostrocaudally, crossing the spanwise elastin bundles (Fig. 6G–I). The most proximal muscle occurs near the elbow, and the rest of the array is a series of similar muscles running parallel to one another in a proximodistal array. The position of the most distal muscle varies: in bats with only a few, closely spaced plagiopatagiales proprii, such as many vespertilionids, the most distal muscle generally occurs just distal to the elbow (Fig. 1A,E); in species with more muscle bellies and/or wider spacing, the muscles repeat across the entire distal span of the plagiopatagium (e.g. Fig. 4F). Where muscles are closely

adjacent to digit V, muscle belly morphology is particularly distinct from the rest of the array and muscles are often especially short (~ 10% of the chord length, e.g. Fig. 4L). In some cases, the distal muscles occur in a paired geometry, with a second muscle belly found along a single rostrocaudal axis, as if a single long muscle was partitioned into more rostral and more caudal elements. In contrast, typical plagiopatagiales proprii are long and occupy ~ 50–75% of the rostrocaudal or chordwise length of the plagiopatagium. Every specimen we examined possessed plagiopatagiales proprii; the number of muscle bellies varied from four to more than 100. In species with many muscle bellies, the comparatively small plagiopatagiales proprii formed essentially a muscular sheet. This sheet-like morphology was not restricted to a single family; it occurred in *Epomops franqueti* (Pteropodidae), *Anoura geoffroyi* (Phyllostomidae), and all Molossidae we examined (Fig. 4F).

Cubitopatagiales

The proximal attachments of the cubitopatagiales were in the region of the elbow. In some species, this muscle was difficult to observe because it was extremely short. We observed between one and eight cubitopatagiales muscles per wing. These muscles run laterally and often span less than one-fourth of the distance from the elbow to digit V. When only a single muscle belly is present, it frequently originates from the elbow in combination with a neurovascular bundle (Figs 4 and 5D). We did not observe any cubitopatagiales in Pteropodidae, Megadermatidae, Furipteridae, and Rhinolophidae. We could not determine whether cubitopatagiales occur in Mystacinidae due to the skin sheath that obscures the elbow in this taxon. Finally, in Rhinopomatidae we observed a distinctive muscle pattern in this region that may not be homologous to the cubitopatagiales muscle arrays in other bats; this array originates from the elbow and runs caudally to the trailing edge of the plagiopatagium, and is similar in length, density, and width to the plagiopatagiales proprii and coracopatagiales.

Discussion

The bilayered skin of all bat wing membranes possesses abundant elastin bundles, muscles, neurovascular bundles, and bundles of organized collagen, in addition to bones and the major skeletal muscles that actuate them. Cross-polarized light imaging, combined with histology, allows us to assess the architecture of these key structural elements in numerous specimens in a manner that is efficient and that accurately identifies specific structures. Our exploration of the wing membranes of 130 species from 17 families of Chiroptera reveals that all bat wings contain arrays of elastin bundles and intramembranous muscles within the wing membrane skin, that the arrangements of elastin bundles and muscle bellies are diverse across Chiroptera, and that species within a single family tend to possess similar

architecture but do not share the same pattern uniformly. In all bats, elastin bundles are oriented predominantly proximodistally, along the wingspan. Of the five anatomically distinct groups of intramembranous muscles in bat wings, we consistently found three of these muscle arrays in all species we examined (Table S1). Within this basic conservation of structural design, however, we observed that the morphology of each array varies substantially; some arrays vary in muscle length and number by more than an order of magnitude. The ubiquity of these structural characteristics, in combination with evidence that muscles in the wing membrane skin are active elements of the bat flight control system (Cheney et al. 2014) and that the elastin bundles are a primary driver of the distinctive mechanical properties of wing skin (Cheney et al. 2015) lead us to conclude that these features play important roles in flight dynamics. Just as other aspects of functional anatomy compel attention in the comparative biology of bats, the structural design of the constituents of wing skin is a subject that demands further investigation for those who seek to understand the mechanistic basis of bat flight, as well as its evolutionary origins and diversification.

Elastin architecture, diversity, and functional significance

The greater diversity of elastin bundle architecture among than within families suggests that elastin network architecture was driven by evolution during the divergence of bat lineages. This is evidenced by differences in bundle density, branching frequency, and anatomical orientation of elastin bundles, as well as in the incidence of both parallel and orthogonal arrays. We observed elaborate networks of elastin bundles in both the plagiopatagium and dactylopatagium in all bat species, although the geometry of bundle interconnections can differ in these two regions of the wing (Fig. 4; Schumacher, 1932; Holbrook & Odland, 1978). However, at the most fundamental level, the elastin bundle architecture in bat wings is a parallel-fibered network oriented along the wing folding/unfolding axis, and the diversity of patterns we observed can be regarded as variations on this 'theme' at fine spatial and taxonomic scales (Fig. 4).

Elastin is ubiquitous in mammalian skin, and although it is typically in small fibril form (one to two orders of magnitude smaller in diameter than bundles in bat wing membranes; Meyer et al. 1994), it plays an important mechanical role by increasing extensibility (Oxlund et al. 1988). In bat wings, spanwise elastin bundles might, therefore, play a critical role in flight dynamics by similarly mediating extensibility. As the wings, including specifically the wing skin, are unfolded early during downstroke, elastin is crucial to skin unfolding in the spanwise direction and facilitates skin deformation as the wings experience aerodynamic forces (Fig. 7). When the wing joints flex during upstroke, the elastin bundles likely maintain tension on the membrane,



Fig. 7 Flying bat imaged at mid downstroke. Wing membrane billows in response to aerodynamic load. Striations in membrane are primarily muscles and elastin bundles. Bat species: *Artibeus jamaicensis* (Phyllostomidae).

reducing flutter and the associated increase in drag (Hu et al. 2008). To establish whether elastin bundles function in this way during flight will require further detailed study of their micro-scale mechanics during natural or naturalistic flight. However, the consistent pattern we observed in the wing elastin architecture suggests that spanwise elastin is functionally important.

In the absence of detailed knowledge of the function of the predominantly parallel, spanwise arrangement of elastin bundles, the functional significance of deviations from this pattern is not clear. Wing membrane skin is highly anisotropic (Swartz et al. 1996), and the difference in skin stiffness in the proximodistal vs. craniocaudal directions is due primarily to organized elastin bundles and not the mechanical properties of the matrix that surrounds them (Cheney et al. 2015). In some species, some regions of the wing possess elastin bundles arranged orthogonally, in addition to the basic, simpler pattern of primarily parallel proximodistal networks (Fig. 4F), or, alternatively, may form honeycomb-like patterns (Fig. 4D, between digits IV and V). We hypothesize that these specific patterns of elastin architecture reduce anisotropy in the mechanical behavior of the wing skin, which, in turn, influences the function of wing skin as the primary component of compliant, deformable airfoils in bats. Anisotropy in compliant wings can influence not only lift-to-drag ratio, but also the degree and chordwise location of maximum camber (Abudaram, 2009; Tanaka et al. 2015), hence variation in elastin geometry that influences anisotropy will almost certainly have aerodynamic consequences. Given the complexity of aerodynamic force production in compliant, flapping airfoils, however, it is not yet possible to confidently predict structure/function relationships. Although it is not presently obvious where or whether specific functional benefits arise from variations in elastin architectural patterns such as honeycomb geometry or orthogonal grids, identification of these distinctive patterns is a valuable step in the development of research agendas, particularly where there is clearly much to be learned.

Plagiopatagium muscle: function, architecture, and diversity

The plagiopatagiales proprii likely serve to stiffen the wing membrane and control wing shape during flight. Their placement and architecture are well suited to this hypothesized function, and direct measurement by electromyography demonstrates that they are active during downstroke in level flight (Cheney et al. 2014). From architecture alone it is not clear whether other wing membrane muscles share a similar functional role. An idealized 1-D model of muscle plus wing membrane skin suggests that relative length of a plagiopatagiales-like muscle to the wing chord is a key factor in the capacity of the model muscle to reduce overall compliance of the wing membrane (Cheney et al. 2014). The cubitopatagiales and tibiopatagiales, the muscles oriented proximodistally, vary in length relative to wingspan by an order of magnitude (Fig. 3), and the 1-D model suggests that at the short end of this range, muscles or muscle arrays are limited in their ability to modulate membrane compliance because of limited control of the wing area. In addition, not only do cubitopatagiales and tibiopatagiales tend to be short, these two muscle groups are also the two least common in the bats in our study sample (absent in five of 17 and seven of 17 families, respectively; Table S1). In contrast, the chordwise-oriented muscles, dorsopatagiales, coracopatagiales, and plagiopatagiales proprii, tend to occupy the majority of the chord length of the plagiopatagium and are found in nearly all families; the single exception is that the coracopatagiales were not observed in *Mystacinidae*. Moreover, for any species, proximodistal spacing between discrete muscle bellies tends to be similar in these three muscle arrays. The dorsopatagiales, coracopatagiales, and plagiopatagiales proprii might thus share similar function, based on this common pattern of occurrence, orientation, size, and spacing. In contrast, the tibiopatagiales and cubitopatagiales may have a different or complementary role. Alternatively, they may act in a manner that is similar to the muscles running in the chordwise direction, but at a reduced functional capacity in those species in which they are relatively short. In this scenario, a small contribution from tibiopatagiales/cubitopatagiales may have little negative consequence if these muscles are usually recruited as part of widespread activation of intramembranous muscles, in synchrony with other muscle groups. Anatomical analysis alone cannot resolve these questions. To distinguish among these hypotheses requires *in vivo* assessment of activation patterns of these muscles by electromyography, preferably in multiple species that represent the diversity of muscle geometry. Such studies are, by their nature, technically challenging; recording activity patterns from very small muscles embedded in compliant skin during flapping flight is extremely difficult. As instrumentation continues to advance in sophistication, we predict that the feasibility of research of this kind will improve.

Cross-polarized light imaging for wing membrane studies

Cross-polarized light imaging is fast, inexpensive, and relatively easy to implement. These traits make it an excellent complement to more detailed but time-consuming, resource-intensive, and/or destructive approaches such as dissection and histology. The wing membrane elastin bundles and muscles can be readily differentiated by their distinct morphology and birefringence in cross-polarized light (Figs 1, 2 and 6G–I). Further, this technique is effective for distinguishing tissues that are neither muscle nor elastin, and/or for targeting structures for further investigation. Without this mode of efficient, non-invasive analysis, rigorous comparative analysis of the structural architecture of wing membrane skin is daunting. Cross-polarized light imaging allows researchers to obtain an overview of structural components in the wing of a specimen in a few hours rather than several weeks, thereby expanding possible sample sizes many-fold. By combining analyses of wing membrane architecture using cross-polarized light imaging with phylogenetically rigorous comparative analysis, histology, and mechanical testing, we can aspire to better understand the wing membrane microstructure, mechanical behavior, and evolution.

A common language for wing membrane muscle anatomy

Over nearly 150 years, many authors have described the muscles of the wing membrane, but the naming and categorization schemes that have been employed to date are inconsistent and, in some cases, contradictory (Table 2; Humphry, 1869; Schöbl, 1871; Macalister, 1872; Maisonneuve, 1878; Morra, 1899; Schumacher, 1932; Vaughan, 1959; Mori, 1960; Norberg, 1972). Research and discussion on the subject of these muscles requires clear, unambiguous communication, and the nomenclature, definitions, and hypotheses of homology we propose should assist future dialog. We sorted the muscle arrays into five groups that are broad enough to be applicable across Chiroptera but fine enough to resolve differences in architectural features of the array. The anatomical names we propose overlap substantially with previous nomenclature and we detail the relationship between the names we propose here and prior usage (Table 2) (Humphry, 1869; Schöbl, 1871; Macalister, 1872; Maisonneuve, 1878; Morra, 1899; Schumacher, 1932; Vaughan, 1959; Mori, 1960; Norberg, 1972). Where we suggest name modifications, we expand the generality of the site of origin to capture the diversity of muscle form across Chiroptera, and describe the insertion site consistently as the 'patagium', illustrated by our suggested replacement of 'tarsocutaneous' with 'tibiopatagialis'. We retain the name 'coracopatagiales' because the origin for this muscle group has been consistently described as the coracoid process of

Table 2 Nomenclature of wing membrane muscles placed within the context of the nomenclature we adopt. Columns indicate families studied, and muscle groups with proposed nomenclature. Rows are publications indicating assignment of reorganized groupings.

	Families studied	Dorsopatagiales	Coracopatagiales	Tibiopatagiales	Cubitopatagiales	Plagiopatagiales proprii
Humphry (1869)	Pt	Branch of Cutaneo-pubic	Coraco-cutaneous			
Schöbl (1871)	Ve	#2	One branch of #1	#4,6,7	One branch of #1	#3
Macalister (1872)	Pt, Ve, Rh, Ph, Mg	Dorsi patagialis	Coraco-cutaneous			
Maisonneuve (1878)	Ve		Coraco-cutane	Tibio-cutane externe		
Morra (1899)	Ve, Rh	Fasci perpendicolari al corpo	Coraco-cutaneo	(1) Tibio-cutaneo esterno; (2) Tarso-cutaneo; (3) Digito-cutaneo; (4) Muscoli cutanei esterni della gamba; (5) Fasci paralleli al corpo	Fascio che accompagna l'arteria ascellare	Fasci verticali del plagiopatagio
Schumacher (1932)	Pt	Dorso-plagiopatagialis; Plagiopatagiales proprii 1–3	Coraco-plagiopatagialis			Plagiopatagiales proprii 4–12
Vaughan (1959)	Ve, Ph, Mo		Coraco-cutaneous	Tensor plagiopatagii	Humeropatagialis	
Mori (1960)	Pt	Dorso-plagiopatagialis; Plagiopatagiales proprii 1–4	Coraco-plagiopatagialis			Plagiopatagiales proprii 5+
Norberg (1972)	Pt	Dorso-plagiopatagialis	Coraco-cutaneous			Plagiopatagiales

Family abbreviations: Mg, Megadermatidae; Mo, Molossidae; Ph, Phyllostomidae; Pt, Pteropodidae; Rh, Rhinolophidae; Ve, Vespertilionidae.

the scapula, although we can only confirm that the origin is in the vicinity of the axilla without detailed and destructive dissections (Maisonneuve, 1878; Morra, 1899; Vaughan, 1959). It is possible, however, that there is variation in this character that has yet to be explored.

The nomenclature we propose will reduce potential confusion that arises when similar names are used to describe distinct muscles and arrays. As an example, 'humeropatagialis' (Vaughan, 1959) could understandably be confused for 'o'mero-cutaneo' or 'humero-cutané' (Maisonneuve, 1878; Morra, 1899), which, despite similar descriptions of origin and insertion site, are quite different. 'O'mero-cutaneo' and 'humero-cutané' describe an array of extremely short muscles (< 5% of the wing chord) arising from the humerus and triceps that extend a short distance into the plagiopatagium and run toward the femur, whereas Vaughan's 'humeropatagialis' matches our description of cubitopatagiales (Table 2). We did not observe wing membrane birefringence consistent with extremely short muscles arising from the humerus; however, this array can appear

continuous with longer forms of the tibiopatagiales, which share a common wing region and path (Morra, 1899).

Framework for future studies

The diversity in elastin and muscle bundle architecture highlights many questions to be addressed about tissue scaling, arrangement, function, and evolution. Future studies could examine whether the large-scale variation in muscle number and size, and/or elastin bundle density, relates to body size and wing loading. Muscle force scales with cross-sectional area, and isometric scaling of total intramembranous muscle cross-sectional area would suggest reduced relative importance of these muscles in larger species. Increase in number or average cross-sectional area may be two alternative evolutionary responses to increase total muscle area. Density in elastin bundle architecture is similarly variable (e.g. relatively low, as in most Vespertilionidae, Fig. 1E or high, as in many Molossidae, Fig. 4E). Elastin bundle density will affect material behavior of the wing membrane,

and high density might provide increased tension, particularly during periods of increased membrane slack, such as upstroke. Elastin density and geometry is also likely to influence skin toughness, including resistance to propagation of tears. An explicitly phylogenetic approach to the diversity of structure in wing membrane architecture could shed light on whether elastin bundle density is driven by ecology/habitat or aerodynamics/kinematics, or might suggest alternative functional roles for elastin bundles.

Regardless of tissue scaling, multiple aspects of wing function that arise from muscle and elastin bundle architecture will differ among Chiroptera. Future functional studies of elastin architecture might explore whether elastin bundles inhibit tear propagation, and whether variation in elastin orientation affects membrane anisotropy. Functional studies of muscle arrays could examine their muscle spindle density and capacity to act as sensory structures, which could place alternative demands on morphology beyond force generation. Additionally, EMG of multiple arrays could address whether muscle arrays act in synchrony. If so, reduction in force capacity of one array may be compensated for through an increase in another, and therefore many muscle architectures may generate an equivalent, or nearly equivalent, effect.

Conclusion

Wing membranes of all bats possess an elaborate network of macroscopic elastin bundles and muscles. This strongly suggests that the ancestor to all modern bats possessed these same architectural elements within the wing membrane. Muscle within the plagiopatagium (armwing) is ubiquitous and its abundance and persistence suggests a critical functional role. However, variation in muscle number and length across taxa suggests that the relative importance of muscle groups probably varies. Future functional studies therefore may have to account for muscle architecture when examining the role of muscles in flight. However, the passive mechanics of elastin within wing membranes, which has been thoroughly explored only in a phyllostomid, is likely similar in all Chiroptera, but the forces generated due to elastin effects and the degree of mechanical anisotropy probably vary among wing regions. By improving understanding of the variation in muscle and elastin architecture in bat wing skin, we can now begin to compose meaningful evolutionary hypotheses, and the tool of cross-polarized light imaging can support those studies by providing morphological insight.

Acknowledgements

Tissue from *T. brasiliensis* was generously donated by Dr. Michael Smotherman. We are grateful to Dr. A. M. Kuzirian and G. R. R. Bell

for histology advice. Rosalyn Price-Waldman assisted with specimen photography. We thank Andrew Bearnot and Elissa Johnson for many helpful discussions. Suggestions from two reviewers substantially improved the final version of this paper. This work was supported by the Bushnell Research and Education Fund to J.A.C., NSF IOS 1145549 and AFOSR FA9550-12-1-0301 DEF, monitored by Patrick Bradshaw, to S.M.S.

References

- Abudaram YJ (2009) Wind tunnel testing of load-alleviating membrane wings. M.S. thesis, Gainesville: University of Florida.
- Cheney JA, Konow N, Middleton KM, et al. (2014) Membrane muscle function in the compliant wings of bats. *Bioinspir Biomim* **9**, 025007.
- Cheney JA, Konow N, Bearnot A, et al. (2015) A wrinkle in flight: the role of elastin fibres in the mechanical behaviour of bat wing membranes. *J R Soc Interface* **12**, 20141286.
- Crowley GV, Hall LS (1994) Histological observations on the wing of the grey-headed flying fox (*Pteropus poliocephalus*) (Chiroptera: Pteropodidae). *Aust J Zool* **42**, 215–231.
- Dimery NJ, Alexander RM, Deyst KA (1985) Mechanics of the ligamentum nuchae of some artiodactyls. *J Zool* **206**, 341–351.
- Fenton MB, Simmons NB (2014). *Bats: A World of Science and Mystery*. Chicago: University of Chicago Press.
- Garvey W, Jimenez C, Carpenter B (1991) A modified Verhoeff elastic-van Gieson stain. *J Histotechnol* **14**, 113–115.
- Gosline J, Lillie M, Carrington E, Guerette P, Ortlepp C, Savage K (2002) Elastic proteins: biological roles and mechanical properties. *Phil Trans R Soc Lond B* **357**, 121–132.
- Gray P (1954) *The Microtome's Formulary and Guide*. New York: Blakiston.
- Gunnell GF, Simmons NB (2005) Fossil evidence and the origin of bats. *J Mamm Evol* **12**, 209–246.
- Gupta BB (1967) The histology and musculature of plagiopatagium in bats. *Mammalia* **31**, 313–321.
- Hedenström A, Johanssen LC (2015) Bat flight: aerodynamics, kinematics and flight morphology. *J Exp Biol* **218**, 653–663.
- Holbrook KA, Odland GF (1978) A collagen and elastic network in the wing of the bat. *J Anat* **126**, 21–36.
- Hu H, Tamai M, Murphy JT (2008) Flexible-membrane airfoils at low Reynolds numbers. *J Aircr* **45**, 1767–1778.
- Humason GL (1962) *Animal Tissue Techniques*. 2nd edn. San Francisco: W.H. Freeman & Co.
- Humphry GM (1869) The myology of the limbs of Pteropus. *J Anat Physiol* **3**, 294–491.
- Macalister A (1872) The myology of the cheiroptera. *Philos Trans R Soc Lond B Biol Sci* **162**, 125–171.
- Madej JP, Mikulová L, Gorošová A, et al. (2013) Skin structure and hair morphology of different body parts in the Common Pipistrelle (*Pipistrellus pipistrellus*). *Acta Zool* **94**, 478–489.
- Maisonneuve P (1878) *Traité de l'ostéologie et de la myologie du Vespertilio murinus, précédé d'un exposé de la classification des chéiroptères et de considérations sur les moeurs de ces animaux*. Paris: Ed: Doin.
- Meyer W, Neurand K, Schwarz R, et al. (1994) Arrangement of elastic fibres in the integument of domesticated mammals. *Scanning Microsc* **8**, 375–390.
- Mori M (1960) Muskulatur des *Pteropus edulis*. *Okajimas Folia Anat Jpn* **36**, 253–307.

- Morra T** (1899) I muscoli cutanei della membrana alare dei chiroteri. *Bull Mus Zool Ed Anat Comp R. Univ Di Torino* **XIV**, 1–7.
- Norberg UM** (1972) Functional osteology and myology of the wing of the dog-faced bat *Rousettus aegyptiacus* (É. Geoffroy) (Mammalia, Chiroptera). *Z Morphol Tiere* **73**, 1–44.
- Norberg UM, Rayner JMV** (1987) Ecological morphology and flight in bats (Mammalia; Chiroptera): wing adaptations, flight performance, foraging strategy and echolocation. *Philos Trans R Soc Lond B Biol Sci* **316**, 335–427.
- Oxlund H, Manschott J, Viidik A** (1988) The role of elastin in the mechanical properties of skin. *J Biomech* **21**, 213–218.
- Sankaran V, Walsh JT Jr, Maitland DJ** (2002) Comparative study of polarized light propagation in biologic tissues. *J Biomed Optics* **7**, 300–306.
- Schöbl J** (1871) Die Flughaut der Fledermäuse, namentlich die endigung ihrer Nerven. *Arch Mikrosk Anat* **7**, 1–31.
- Schumacher S** (1932) Muskeln und Nerven der Fledermaus-flughaut. *Anat Embryol* **97**, 610–621.
- Shadwick RE, Goldbogen JA, Potvin J, et al.** (2013) Novel muscle and connective tissue design enables high extensibility and controls engulfment volume in lunge-feeding orqual whales. *J Exp Biol* **216**, 2691–2701.
- Shi JJ, Rabosky DL** (2015) Speciation dynamics during the global radiation of extant bats. *Evolution* **69**, 1528–1545.
- Sokolov VE** (1982) *Mammal Skin*. Berkeley: University of California Press.
- Swartz SM, Konow N** (2015) Advances in the study of bat flight: the wing and the wind. *Can J Zool* **93**, 977–990.
- Swartz SM, Groves MS, Kim HD, et al.** (1996) Mechanical properties of bat wing membrane skin. *J Zool* **239**, 357–378.
- Tanaka H, Okada H, Shimasue Y, et al.** (2015) Flexible flapping wings with self-organized microwrinkles. *Bioinspir Biomim* **10**, 46005.
- Teeling EC, Springer MS, Madsen O, et al.** (2005) A molecular phylogeny for bats illuminates biogeography and the fossil record. *Science* **307**, 580–584.
- Vaughan T** (1959) Functional morphology of three bats: *Eumops*, *Myotis*, *Macrotus*. University of Kansas Publications, Museum of Natural History **12**, 1–153.
- Weaver HL** (1955) An improved gelatin adhesive for paraffin sections. *Biotech Histochem* **30**, 63–64.
- Wilson DE, Reeder DM** (2005) *Mammal Species of the World. A Taxonomic and Geographic Reference*, 3rd edn. Baltimore: Johns Hopkins University Press.

Supporting Information

Additional Supporting Information may be found in the online version of this article:

Table S1. Summary of the range of muscle array number and/or length observed within families. Phylogeny from Teeling et al. (2005).